

Comparative Study of Single and Double Hybrid Density Functionals for the Prediction of 3d Transition Metal Thermochemistry

Wanyi Jiang, Marie L. Laury, Mitchell Powell, and Angela K. Wilson*

Department of Chemistry and Center for Advanced Scientific Computing and Modeling (CASCAM), University of North Texas, Denton, Texas 76203-5017, United States

S Supporting Information

ABSTRACT: The performance of 13 density functionals, including hybrid-GGA, hybrid-meta-GGA, and double-hybrid functionals, in combination with the correlation consistent basis sets, has been evaluated for the prediction of gas phase enthalpies of formation for a large set of 3d transition-metal-containing molecules with versatile bonding features. Of the methods studied, the hybrid B97-1 functional and the double hybrid functional mPW2-PLYP exhibit the best overall performance with mean absolute deviations (MAD) from experimental data of 7.2 and 7.3 kcal mol⁻¹, respectively. For single reference molecules, where dynamic correlation predominates, the results of the hybrid functionals B97-1, B98, and ω B97X and the double hybrid functionals B2-PLYP, B2GP-PLYP, and mPW2-PLYP yield the smallest deviations from the experimental enthalpies of formation. For the prediction of thermodynamic properties of coordination complexes including metal carbonyls, B97-1 and mPW2-PLYP are the most promising functionals of those investigated. When the size of the molecule is considered, B97-1 and B98 outperform mPW2-PLYP for diatomics and triatomics, while mPW2-PLYP yields the lowest MAD for larger molecules.

1. INTRODUCTION

Density functional theory (DFT) is a popular approach due to its demonstrated predictive abilities for a wide range of chemical systems and properties and relatively low computational cost as compared to wave-function-based methods. DFT has been employed for gas phase predictions of transition metal (TM) properties¹ such as equilibrium geometries,^{2–8} the determination of electronic ground states,^{9–16} ionization potentials,^{13–17} and reaction enthalpies.^{18–24} Despite the continuous development of new functionals and the broad application of DFT, the quantitative performance of DFT for energetic and thermodynamic properties of transition-metal-containing systems has been gauged much less than for main group species. It has been recognized that functionals that perform best for main group species may not necessarily result in the most reliable predictions for TM species,^{25–27} and thus comparative studies of the performance of density functionals for the prediction of properties such as the thermochemistry of TM species are imperative.

There have been a number of benchmark studies of functional performance for the energetics of TM species. For example, Grimme et al. compared double hybrid density functionals (PWBPB95, PTPSS, B2-PLYP, B2GP-PLYP, DSD-BLYP, and XYG3) for the prediction of reaction enthalpies for the first CO dissociation of transition metal carbonyls Cr(CO)₆, Fe(CO)₅, and Ni(CO)₄.²⁸ Furche and Perdew investigated the performance of several density functionals (LSDA, BP86, PBE, TPSS, B3LYP, and TPSSH) for the prediction of properties including the dissociation energies of diatomics (i.e., homologous dimers, hydrides, monofluorides, monoxides, and nitrides of 3d transition metals), as well as the enthalpies of 14 dissociation reactions of coordination complexes.²⁷ In these studies, the prediction of dissociation

energies, bond enthalpies, or reaction enthalpies were compared, where there may be significant cancellation of errors due to the similarity of electronic structures between reactant and product molecules.^{7,8,18,20,25,27}

The calculation of atomization energies, or enthalpies of formation (ΔH_f) via atomization energies, on the contrary, can be challenging for density functionals as a result of the strikingly different electron density between molecules and their constituent atoms, and these differences can be quite substantial for transition metal species and can result in very large errors in the prediction of atomization energy-based properties. For example, deviations from experimental results ranged from a few kilocalories per mole to over 100 kcal mol⁻¹ for the widely used B3LYP functional used with both the Los Alamos (LANL) and the Stevens (CEP) effective core potentials when determining ΔH_f via atomization energies for a set of 26 TM molecules in a study by Cundari and co-workers.²⁹ The observed large deviations help to illustrate the potential sensitivity of an atomization energy-based ΔH_f with respect to functional/basis set choice for transition metal species and have sparked subsequent interest in identifying better performing density functional and basis set (or effective core potential)³⁰ combinations for the determination of properties such as ΔH_f for transition metal species.

Progress has been made in the systematic assessment of the performance of various density functionals by employing diverse molecule sets for the calculation of ΔH_f 's for TM species. Riley and Merz investigated nine density functionals for the prediction of the ΔH_f of 94 TM molecules using all electron basis sets (6-31G** and TZVP)³¹ and mixed basis sets

Received: June 1, 2012

(6-31G**) with effective core potentials (LANL2DZ).³² Among the density functionals investigated, TPSS1KCIS,^{33,34} a hybrid-meta-generalized gradient approach (GGA), resulted in the smallest mean absolute deviation (MAD) of 9.1 kcal mol⁻¹ when compared to experimental data (or 7.9 kcal mol⁻¹ when compared to updated experimental data³⁵). The experimental uncertainties for the 94 ΔH_f° 's span from less than 1.0 kcal mol⁻¹ to 10.0 kcal mol⁻¹. The presence of large experimental uncertainties can mask the statistical results, preventing a precise assessment of the quality of the functionals. Additionally, no molecules containing scandium were considered in the study of Riley and Merz. Dixon et al.²² compared the performance of 27 density functionals to wave function-based theory, coupled cluster including singles, doubles, and perturbative triples [CCSD(T)], for the prediction of atomization energies and ΔH_f° 's of group IVB and VIB transition metal oxide clusters. Our group has investigated 44 functionals with both cc-pVTZ and cc-pVQZ basis sets.³⁶ The 19 molecules considered in the study all had small (for transition metal species) experimental uncertainties (± 3.0 kcal mol⁻¹ or less).³⁷ It was concluded that the appropriate hybridization of nonlocal Hartree–Fock (HF) exchange is essential for the overall accuracy of the functional, consistent with earlier findings by Truhlar and co-workers^{25,26,38} and by Riley and Merz.³¹ In our earlier study,³⁶ a surprisingly low MAD, 3.1 kcal mol⁻¹, with respect to experimental results was obtained using B97-1³⁹ in combination with the cc-pVQZ basis set. While the study demonstrated that density functionals, such as B97-1, show promise as a computationally inexpensive method for the prediction of ΔH_f° 's, the 19-molecule set considered did not contain enough molecules to gauge functional performance, and the set was lacking in terms of the diversity of molecular bonding type (e.g., bonding in metal oxides, halides, and carbonyls, and single, double, triple bonds). It is thus important to further examine the best-performing functional, B97-1, from our earlier study, as well as consider closely related variants of B97-1, on a larger set of molecules with a variety of bonding properties.

For main group chemistry, there are a number of widely popular sets of thermochemical data that have small (<1.0 kcal mol⁻¹) experimental uncertainties and can be used to gauge the performance of theoretical approaches. The most notable examples are the G2/97⁴⁰ and G3/05⁴¹ sets, which include enthalpies of formation, proton affinities, and electron affinities. However, for transition metal thermochemistry, where the very best reported gas phase experimental uncertainties are, on average, much larger than for main group species and where the data that are available are much more sparse, such data sets that can be used for gauging the performance of theoretical methods are much less prevalent. This is particularly true for ΔH_f° 's. Truhlar et al. developed a set of nine atomization energies of metal dimers,²⁶ 21 bond dissociation energies,²⁵ and 18 reaction energies^{20,27} for TM and used the atomization energies and dissociation energies for the development and assessment of the Minnesota family of density functionals, including M06.³⁸ Mayhall et al. have developed a relatively limited set of 20 ΔH_f° 's of small-sized molecules for the TM variants of the Gaussian-4 method (G4).²³ In their study, several density functionals were compared to G4, and it was noted that B3LYP was in better agreement with experimental results than the pure PW91 and PBE functionals for ΔH_f° 's.

Recently, a set of ΔH_f° 's for 225 3d transition-metal-containing molecules was composed. This set was pruned to

create the ccCA-TM/11 set of 193 molecules, removing molecules with particularly large experimental uncertainties as well as those with possible very strong nondynamical correlation (multireference character), as indicated by the T_1/D_1 , and C_0^2 diagnostics.³⁵ Though the uncertainties in the experimental ΔH_f° 's for some of the molecules in this set are still quite large (as large as 20 kcal mol⁻¹), the set does include ΔH_f° 's with experimental uncertainties of less than 1.0 kcal mol⁻¹. Including such a range of experimental uncertainties was necessary to establish a large, diverse benchmark set. To aid with analysis, however, the ccCA-TM/11 was divided into categories based upon experimental uncertainties. As well, this earlier study also considered the performance of methodologies according to metal centers, bonding types, and multireference character.

Initially, the ccCA-TM/11 set was compiled as a gauge of the performance of a new *ab initio* composite method, the correlation consistent Composite Approach^{42,43} [as modified for transition metal species (ccCA-TM)^{35,44,45}], which was designed in our laboratory. It includes molecules as large as Sc(C₅H₅)₃ and (CrO₃)₃ and various types of molecules such as halides, oxides and heavy chalcogenides, hydrides, nitrides, small clusters, and metal carbonyls and other coordination complexes. ccCA-TM/11 represents the largest and most diverse benchmark set for ΔH_f° 's of 3d transition metal species available to date and will serve as an informative gauge for DFT performance and development. In this work, we will utilize this valuable data set.

In considering functionals to examine for transition metal thermochemistry, functionals based on local spin density approximation (LSDA) severely overestimate bonding energies,⁴⁶ and, thus, pure LSDA functionals were not considered in this study. Corrections of first order density gradients significantly improve the accuracy in describing the inhomogeneous electron density in molecular systems. The inclusion of this correction within a functional results in a GGA functional. Since the hybridization of HF exchange has proven to be critical^{25,26,31,36,38} for the overall accuracy of DFT for the prediction of ΔH_f° 's, only hybrid variants of GGA functionals are considered. The single hybrid GGA functionals assessed in this study include B3LYP,⁴⁷ the most popular functional for molecular properties, and the B97⁴⁸ family (B97-1,³⁹ B98,⁴⁹ B97-2,⁵⁰ ω B97 and ω B97X,⁵¹ and ω B97X-D,⁵² see Table 1) due to the superior performance of B97-1 in our earlier study. The introduction of kinetic energy density or the local Laplacian of spin density to the GGA functionals results in a suite of functionals termed meta-GGA. The hybrid-meta-GGA functionals considered in this study are M06,³⁸ PBE1KCIS,⁵³ and TPSS1KCIS.^{33,34} M06 has been parametrized using atomization energies and dissociation energies of TM species, while PBE1KCIS and TPSS1KCIS are representative functionals with no empirical parameters (except one parameter for the HF exchange). The double hybrid density functionals (B2-PLYP and mPW2-PLYP) proposed by Grimme et al.^{54,55} include an MP2-type correlation energy term based on virtual Kohn–Sham (KS) orbitals and are referred to as fifth-rung density functionals on the metaphorical Jacob's ladder of density functionals by Perdew et al.⁵⁶ The B2GP-PLYP functional (“GP” for “general purpose”)⁵⁷ is a reoptimized B2-PLYP functional fit to the W4 theoretical model for both thermochemistry and kinetics. The *ad hoc* treatment of perturbative terms is closely related to the Görling–Levy perturbation theory,⁵⁸ and the global parameters may be

Table 1. A Summary of Functionals Investigated in This Study

functional	type	notes
B3LYP	hybrid GGA	ref 47
B97-1	hybrid GGA	refs 39, 48
B97-2	hybrid GGA	fit with ZMP potential, ref 49
B98	hybrid GGA	parameters optimized using the G2/97 set, ref 50
ω B97	GGA	range separation with long-range HF exchange, ref 51
ω B97X	hybrid GGA	hybrid use of HF and density functional for short range, ref 51
ω B97X-D	hybrid GGA	including one additional dispersion term, ref 52
M06	hybrid meta GGA	fit with TM thermochemical data, ref 38
PBE1KCIS	hybrid meta GGA	ref 53
TPSS1KCIS	hybrid meta GGA	refs 33, 34
B2-PLYP	double hybrid GGA	ref 54
B2GP-PLYP	double hybrid GGA	ref 57
mPW2-PLYP	double hybrid GGA	ref 55

derived by theoretical considerations⁵⁹ instead of fitting with benchmark data. Many double hybrid functionals (see a recent example in ref 28 and references therein) have been developed for main group species with performances superior to their single hybrid counterparts, but their accuracy has not been systematically assessed for TM thermochemistry. A comprehensive assessment of all double-hybrid variants of density functionals²⁸ is beyond the scope of this study, and only the three earlier representative examples, B2-PLYP, B2GP-PLYP, and mPW2-PLYP, were considered herein.

In this study, we assessed the performance of both single hybrid (hybrid GGA and hybrid meta-GGA) and double hybrid density functionals for the prediction of ΔH_f° 's of TM-containing molecules in the ccCA-TM/11 set. To gain an understanding of the impact of basis set choice on two types of functionals, two functionals were considered: the widely popular (and more computationally efficient) GGA functional, B3LYP, and the more recent meta-GGA M06 functional, whose use has been advocated³⁸ in some studies of transition metal species (i.e., atomization energies and dissociation energies of TM species). These two functionals were both partnered with cc-pVTZ and cc-pVQZ basis sets. Though basis set effects on transition metal species have been considered in earlier studies when used in combination with density functionals,³⁶ this has not yet been done for such a large, diverse study of 3d transition metals. Other density functionals in this study were evaluated in combination with the larger cc-pVQZ (or aug-cc-pVQZ) basis set. The results were analyzed according to a number of classifications based upon metal center, single reference/multireference, coordination chemistry, multiplicity (open shell, closed shell), and molecule size.

2. COMPUTATIONAL METHODS

All calculations were performed using the Gaussian 09 suite.⁶⁰ Correlation consistent basis sets^{61–64} of triple- ζ and quadruple- ζ quality were employed. When different theories and/or basis sets were employed for a single-point ΔH_f° calculation than those that were used for the geometry optimization, “//” is

added to separate the methods for the single point energy calculation and the geometry optimization. Herein, however, while all of the single point energy calculations using double hybrid functionals were done using B3LYP/cc-pVQZ geometries, for simplicity, B3LYP/cc-pVQZ was dropped from the notation. Though scale factors for vibrational frequencies of main group species were recently introduced⁶⁵ for all of the functionals in this study, for simplicity, a single scale factor of 0.989, originally optimized for B3LYP/cc-pVTZ for main group species,⁴³ was used for all functionals. Ten functionals (B3LYP, B97-1, B98, ω B97X, M06, TPSS1KCIS, PBE1KCIS, B2-PLYP, B2GP-PLYP, and mPW2-PLYP) were compared to experimental results for the predictions of ΔH_f° using the cc-pVQZ basis set. For each functional in the B97 family of functionals (B97-1, B97-2, ω B97, ω B97X, and ω B97X-D), aug-cc-pVQZ single-point calculations were conducted at the aug-cc-pVTZ geometry (i.e., B97-1/aug-cc-pVQZ//B97-1/aug-cc-pVTZ, B97-2/aug-cc-pVQZ//B97-2/aug-pVTZ). “Fine” grids were applied to all calculations in this study. However, to assess the impact of grid choice for calculations on transition metal species, “ultrafine” grids were also utilized for the B97/aug-cc-pVQZ//B97/aug-cc-pVTZ calculations. The ΔH_f° 's were calculated via the standard atomization energy-based approach,⁶⁶ where the experimental data for the atomic ΔH_f° 's was used. A detailed description of the experimental data for the ground states and their sources can be found in ref 35. Spin-orbit corrections³⁵ were considered in the calculations of ΔH_f° 's. For 3d transition metal atoms, the lowest atomic energies predicted by each density functional and basis set combination were used.^{20,67}

3. RESULTS AND DISCUSSION

3.1. Basis Set Effects. Our earlier study³⁶ showed that the utilization of the cc-pVQZ basis set reduced the MAD of all 23 hybrid functionals considered in the study by 1.2–4.1 kcal mol^{−1} compared to the cc-pVTZ basis set. In the study of Riley and Merz,³¹ significant decreases in MAD were also found for three meta-GGA functionals, TPSS1PSS, TPSS1KCIS, and BB95, when the TZVP basis set was used instead of 6-31G**. Similar to these previous studies, a consistent decrease in MAD was found for B3LYP when the basis set size increased from cc-pVTZ to cc-pVQZ for all molecule sets given in Table 2. However, the decrease in MAD is not as pronounced as in our earlier study. Here, the difference in B3LYP MAD for the overall set is 0.3 kcal mol^{−1}. To aid in analysis, the ccCA-TM/11 has been divided into subsets, based upon experimental uncertainties (i.e., ≤ 1.0 , ≤ 2.0 , ≤ 3.0 , ≤ 4.0 , and ≤ 5.0 kcal mol^{−1}, see Table 2). To note, subsets with larger experimental uncertainties are inclusive of smaller subsets; i.e., the subset of ≤ 2.0 kcal mol^{−1} includes all species in the subset of ≤ 1.0 kcal mol^{−1}, as well as species with experimental uncertainty of 1.0–2.0 kcal mol^{−1}; the subset of ≤ 3.0 kcal mol^{−1} includes all species in the subset of ≤ 2.0 kcal mol^{−1}, as well as species with experimental uncertainty from 2.0–3.0 kcal mol^{−1}; and so forth. In the following discussion of the B3LYP results, the subset distinctions are omitted due to the small differences (<1.2 kcal mol^{−1}) in MADs across the subsets. Similarly, for the M06 functional, the differences in MAD are in the range of 0.1–0.5 kcal mol^{−1} for all subsets.

To examine the basis set effect (cc-pVTZ versus cc-pVQZ) for the B3LYP and M06 calculations, each functional/basis set combination was used for all aspects of the determination of ΔH_f° 's, including the geometry optimization, frequency analysis,

Table 2. B3LYP and M06 Mean Absolute Deviations (MAD; kcal mol⁻¹) of ΔH_f° 's Relative to Experimental Data for 3d Transition Metal Subsets with Increasing Experimental Uncertainties (kcal mol⁻¹)

exptl. uncertainty	≤1.0	≤2.0	≤3.0	≤4.0	≤5.0	overall
# of molecules	32	70	96	116	139	193
B3LYP/cc-pVTZ	13.92	14.13	13.95	13.29	12.94	13.30
B3LYP/cc-pVQZ	13.60	13.61	13.51	12.92	12.64	13.04
M06/cc-pVTZ	10.92	10.84	11.02	10.50	10.60	11.00
M06/cc-pVQZ	10.42	10.64	10.94	10.40	10.61	11.07
deviations of MADs when using B3LYP/cc-pVTZ geometries ^a						
B3LYP/cc-pVQZ	-0.07	-0.06	+0.08	+0.07	+0.05	+0.01
M06/cc-pVTZ	+0.09	+0.09	+0.03	+0.03	+0.04	+0.00
M06/cc-pVQZ	+0.06	+0.06	+0.01	+0.00	+0.01	-0.02

^aSingle point energy calculations were performed at B3LYP/cc-pVTZ geometries. Energy differences of the mixed method are given with respect to the original single method.

and energy evaluation. Such comparisons do not tell if the basis set effects originate mainly from the geometries and frequencies, or the single point energies. To further evaluate the basis set effects on ΔH_f° , we obtained single point B3LYP/cc-pVQZ energies at the B3LYP/cc-pVTZ geometries. As expected, the MADs of the mixed B3LYP/cc-pVQZ//B3LYP/cc-pVTZ are within ± 0.1 kcal/mol⁻¹ of the B3LYP/cc-pVQZ MADs, suggesting that the geometry optimization can generally be performed with smaller basis sets without affecting the overall accuracy for TM species, similar to the common observation for main group molecules.⁶⁸

We also considered the replacement of M06/cc-pVTZ or M06/cc-pVQZ by B3LYP/cc-pVTZ in the geometry optimization and frequency calculations. The MADs of the mixed approaches (M06/cc-pVTZ//B3LYP/cc-pVTZ and M06/cc-pVQZ//B3LYP/cc-pVTZ) are within ± 0.1 kcal/mol⁻¹ of the original M06/cc-pVTZ and M06/cc-pVQZ MADs, respectively (Table 2). Consequently, for the systems considered, B3LYP/cc-pVTZ can predict equilibrium geometries and vibrational frequencies of the same quality as those by a more sophisticated and more costly method, such as M06/cc-pVQZ, and it is the level of theory used for the single point energy calculations that determines the accuracy of the calculated ΔH_f° 's.

By using ultrafine grids instead of fine grids in the DFT calculations, differences of less than 0.0001 au in the atomic energies were found for B3LYP/cc-pVTZ and differences of less than 0.0004 au were observed for M06/cc-pVTZ. While the energy differences were greater for the predicted molecular ΔH_f° 's, the deviations proved to be negligible. For example, in the B3LYP/cc-pVTZ calculation for the ΔH_f° of Sc(C₅H₅)₃, the difference between the fine grid and ultrafine grid was 0.08 kcal/mol⁻¹.

3.2. Overall Performance. **3.2.1. The B97 Family of Functionals.** The B97-1 functional, using the cc-pVQZ basis set, yields a MAD of 7.2 kcal/mol⁻¹ for the overall ccCA-TM/11 set, significantly less than the MAD of 13.0 kcal/mol⁻¹ obtained with B3LYP (Figure 1a). The relatively large errors of B3LYP might originate from an overestimation of metal–ligand binding energies by B3LYP, as shown by the overall B3LYP

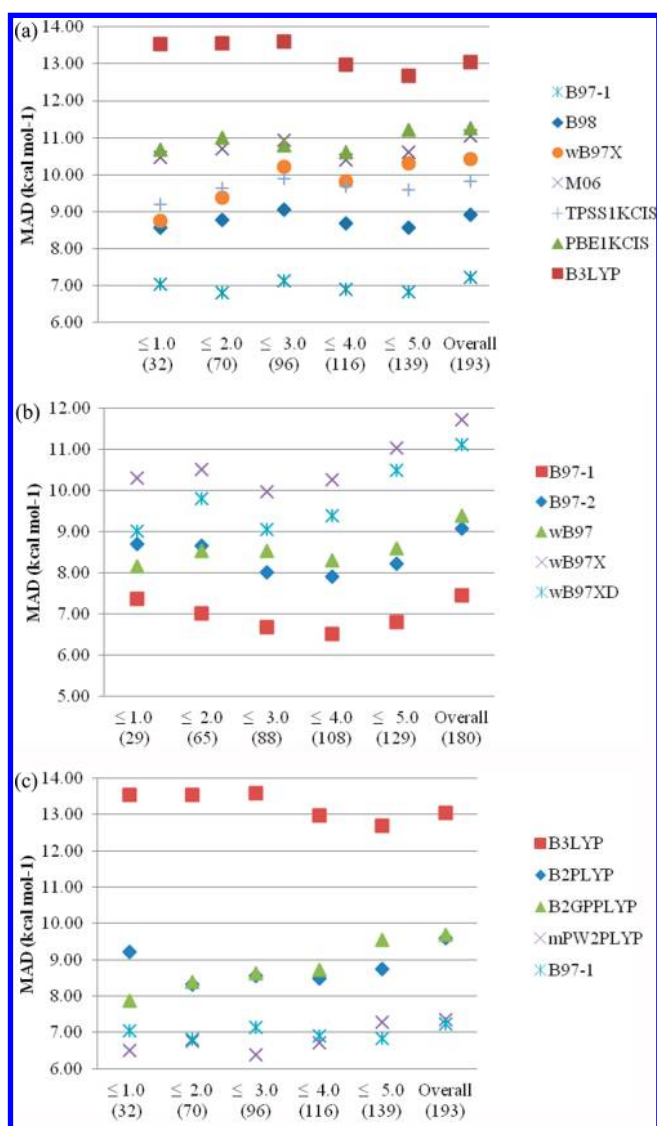


Figure 1. (a) MADs (kcal mol⁻¹) of single hybrid functionals for subsets with increasing experimental uncertainties. (b) MADs (kcal mol⁻¹) of the B97 family of functionals for subsets with increasing experimental uncertainties (13 molecules were removed from the ccCA-TM/11 set due to convergence problems.) (c) MADs (kcal mol⁻¹) of double hybrid functionals (Cr₂ excluded), B3LYP, and B97-1 for subsets with increasing experimental uncertainties.

MSD of -11.1 kcal/mol⁻¹, as compared to the B97-1 MSD of -2.4 kcal/mol⁻¹. When utilizing ccCA-TM for the ccCA-TM/11 set, a monotonic decrease of the MAD is observed as the experimental uncertainty decreases.³⁵ In contrast to the ccCA-TM results, the B97-1 MADs do not show any discernible increasing/decreasing patterns across the subsets of decreasing experimental uncertainty. The B98 functional, sharing the same formulas of B97-1, was reoptimized using the G2/97⁴⁰ set of 148 main group ΔH_f° 's. However, B98 yields larger MADs than B97-1 for the TM systems, and the overall MAD is 8.9 kcal/mol⁻¹, which is 2.7 kcal/mol⁻¹ greater than that of B97-1. The B97-1 and B98 MADs (7.2 and 8.9 kcal/mol⁻¹, respectively) for the ccCA-TM/11 set are much higher than their MADs (3.1 and 6.9 kcal/mol⁻¹, respectively) for the 19-molecule set in our earlier study.³⁶ The substantial increase of the B97-1 MADs from the 19-molecule set to the ccCA-TM/11 set suggests that the assessment of certain functionals may lead to fortuitous

results if the molecule set is limited in size and/or bonding features. The ω B97X functional, containing a long-range correction to the exchange energy, has more empirical parameters (17 parameters) than B97-1 (10 parameters) and outperforms B97-1, for the G3/99 set of 223 main group ΔH_f° 's, by a notable margin (MAD of 2.09 kcal mol⁻¹ vs 4.85 kcal mol⁻¹).⁵¹ However, the modifications in ω B97X deteriorate the overall quality of calculated ΔH_f° 's for TM species considered in this study, yielding an overall MAD of 10.4 kcal mol⁻¹ for the ccCA-TM/11 set.

Due to the promising performance of B97-1, we considered additional variants of the B97 functional, including B97-1, B97-2, ω B97, ω B97X, and ω B97X-D (Figure 1b). To examine the highest level of accuracy obtainable with DFT for transition metals, augmented basis sets (aug-cc-pVnZ, n = T,Q) were utilized in the extended study of the variants of the B97 functional. While the hybrid GGA functionals B97-1 and B97-2 were each fit to energetic data from the G2-1 training set, the B97-2 functional has the additional fitting to a Zhao, Morrison, and Parr (ZMP) exchange-correlation potential derived from *ab initio* Brueckner doubles or MP2 electron densities.⁵⁰ The ω of the ω B97, ω B97X, and ω B97X-D has been used to correct the asymptotic behavior of a pure exchange functional by defining the regions described by the long-range Coulomb operator (Table 1). Three range-separated hybrid functionals based on PBE were compared to other functionals for the predictions of equilibrium geometries and dissociation energies of TM complexes;⁷ however, none of the ω B97, ω B97X, and ω B97X-D functionals have been considered systematically for TM thermochemistry prior to our study. The X in ω B97X and ω B97X-D indicates the inclusion of Hartree–Fock exact exchange in the short-range exchange, and the D represents the inclusion of a dispersion correction within the ω B97X-D functional. For a few of the molecules, severe convergence problems in the calculations were encountered with all or some of the functionals. The absolute deviations of ΔH_f° from experimental data by ω B97X and ω B97X-D were greater than 150 kcal mol⁻¹ for Cr₂. As a result, 13 molecules including Cr₂ were excluded from the ccCA/TM11 set for the B97/aug-cc-pVQZ//B97/aug-cc-pVTZ calculations (Figure 1b). Compared to the B97/cc-pVQZ calculations, the performance of B97-1 was comparable, but the MAD of ω B97X was slightly larger. The increases in MAD are 0.2–0.4 kcal mol⁻¹ for B97-1 and 0.3–1.5 kcal mol⁻¹ for ω B97X.

B97-1 gives the lowest MADs among the five B97 functionals. The parametrization using the ZMP potential in the fitting of the B97-2 functional does not improve the results as compared to B97-1, possibly because the ZMP potential derivation is based upon main group species. The B97-2 MADs show the same patterns across the subsets as those of B97-1 but are 1.4–1.7 kcal mol⁻¹ greater. The long-range corrected ω B97 functional results are inferior to B97-1 (overall MAD of 9.4 kcal mol⁻¹ for ω B97 and 7.5 kcal mol⁻¹ for B97-1) but show improvements over ω B97X (overall MAD of 11.7 kcal mol⁻¹) and ω B97X-D (overall MAD of 11.1 kcal mol⁻¹). The hybrid use of Hartree–Fock exchange for the short-range interactions in ω B97X, where ω already introduces the Hartree–Fock exchange for the long-range interactions, increases the overall MAD for the TM ΔH_f° 's by over 2.5 kcal mol⁻¹. The introduction of a dispersion parameter slightly improves the performance of the long-range corrected hybrid functional for the prediction of TM ΔH_f° 's.

3.2.2. Hybrid-meta-GGA Functionals. The empirical parameters in the M06 functional³⁸ were fit to experimental data including nine atomization energies of metal dimers²⁵ and 21 metal–ligand bonding energies,²⁶ which do not sufficiently reflect the diversity of TM–ligand bonding features; e.g., transition metal halides, polyoxides, or coordination complexes other than carbonyls were omitted in the M06 training set. The generally applicable hybrid-meta-GGA functional, M06, exhibits a better accuracy than B3LYP, but its MADs (e.g., the overall MAD of 11.0 kcal mol⁻¹) for TM ΔH_f° 's are much greater than that of the hybrid GGA functional B97-1 (Figure 1a). The local variant, M06L, although recommended for TM species, is not considered here as an earlier study shows that HF exchange is critical for the reliable prediction of TM ΔH_f° 's by meta-GGA functionals, and M06-L does not include HF exchange.³⁶

Previous studies have shown that the hybridization of HF exchange makes pronounced improvements over the pure functionals TPSSKCIS and PBEPBE;³¹ therefore, the single hybrid-meta-GGA functionals, PBE1KCIS and TPSS1KCIS, with one parameter for HF exchange were considered. The MADs of TPSS1KCIS range from 9.2 to 9.9 kcal mol⁻¹ for the various sets (Figure 1a), consistent with the study of Riley and Merz, where TPSS1KCIS provided a MAD of 9.1 kcal mol⁻¹ for 94 TM molecules. The overall MAD of TPSS1KCIS is slightly better than M06. The PBE1KCIS functional, using the GGA PBE exchange functional instead of the meta-GGA TPSS exchange functional, yields MADs of 10.9–11.7 kcal mol⁻¹, which are 1.4–2.2 kcal mol⁻¹ higher than those of TPSS1KCIS. Similar to B97-1, TPSS1KCIS results in a narrow range of MADs (9.2–9.9 kcal mol⁻¹) across the subsets, supporting that each subset can be used as a diverse benchmark for the evaluation of DFT functionals.

3.2.3. Double-Hybrid Functionals. The double hybrid B2-PLYP has the same Becke exchange and Lee–Yang–Parr correlation functionals as B3LYP, and thus a comparison between B2-PLYP and B3LYP may reveal the effects of the inclusion of MP2-type correlation energy based on KS virtual orbitals. Single reference perturbation theory MP2 fails for multireference systems (see an example in ref 69) where a multiconfigurational reference wavefunction is critical for a qualitatively correct description. For example, very large deviations of 135–195 kcal mol⁻¹ from experimental results were observed for the molecule Cr₂ by the three double hybrid functionals considered in this study. To avoid the large bias introduced by Cr₂, the outlier molecule Cr₂ has been excluded from the subsequent statistical analysis of double hybrid functionals. The overall MAD of B2-PLYP is 10.5 kcal mol⁻¹, compared to the MAD of B3LYP, 13.0 kcal mol⁻¹ (Figure 1c). The B2GP-PLYP reoptimized by Martin and co-workers⁵⁷ gives results similar to B2-PLYP, except that for the subset with experimental uncertainties up to 1.0 kcal mol⁻¹, B2GP-PLYP achieves a lower MAD, 7.9 kcal mol⁻¹, than B2-PLYP, 9.2 kcal mol⁻¹. In a study by Schwabe and Grimme,⁵⁵ mPW2-PLYP showed noticeable improvements over B2-PLYP for the G3/05 set. The overall MAD of mPW2-PLYP is 8.0 kcal mol⁻¹, which is 2.5 kcal mol⁻¹ less than that of B2-PLYP. For the subset of 32 TM molecules with experimental uncertainty of up to 1.0 kcal mol⁻¹, mPW2-PLYP yields a MAD of 6.5 kcal mol⁻¹, compared to the B97-1 MAD of 7.3 kcal mol⁻¹. It should be mentioned that the performance of mPW2-PLYP can be further improved if the core–core and core–valence interactions, which were found important for accurate TM thermochemistry,^{35,45} can be considered in the perturbation energy component.

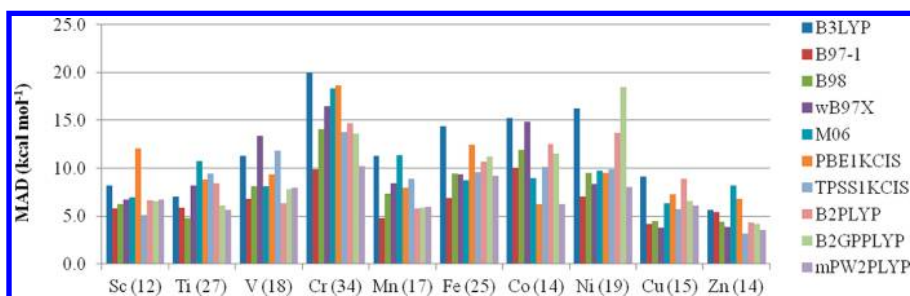


Figure 2. MADs (kcal mol^{-1}) of density functionals for each 3d transition metal center (Cr₂ excluded).

3.3. Bonding Features. The performance of DFT may vary drastically for molecules with different bonding features; e.g., much larger MADs relative to experiments were obtained by density functionals for metal carbonyls than those for simple compounds such as halides and oxides.³⁶ As a result, the performance of functionals is also assessed on the basis of metal center, single reference/multireference character, coordination chemistry, multiplicity (open shell versus closed shell), or the molecular size (the number of atoms).

3.3.1. Metal Centers. The MADs of each density functional vary substantially across the 10 metal centers (Figure 2). The largest MADs were obtained for the chromium set. One exception is B2GP-PLYP, which yields the largest MAD for the nickel molecules. In comparison to the other functionals, B2GP-PLYP shows considerable underestimation of the binding energies for NiO, NiF, and NiBr₂, and the unusual errors may contribute to the large MAD of B2GP-PLYP for nickel-containing molecules. Although B97-1 results in the lowest overall MAD, competitive functionals for each metal center are found. The “best” functionals with the smallest MADs for each metal are TPSS1KCIS for Sc; B98 for Ti; B2-PLYP and B97-1 for V; B97-1 and mPW2-PLYP for Cr; B97-1 for Mn, Fe, and Ni; PBE1KCIS and mPW2-PLYP for Co; ω B97X for Cu; and TPSS1KCIS for Zn. Despite the inclusion of 30 TM data points in the M06 parametrization,³⁸ M06 is the only hybrid-meta-GGA functional that does not give the lowest MAD for any single metal set. M06 results in the second lowest MAD for the iron and cobalt sets but does not exhibit competitive accuracy for any of the other metal centers. Single hybrid functionals, when yielding a comparable accuracy to double hybrid functionals, are preferred since the former are more computationally favorable. The smallest MADs obtainable by density functionals studied herein for each metal are as follows: Zn ~ Cu ($\pm 3\text{--}4 \text{ kcal mol}^{-1}$) < Sc ~ Ti ~ Mn ($\pm 5 \text{ kcal mol}^{-1}$) < V ~ Fe ~ Co ~ Ni ($\pm 6\text{--}7 \text{ kcal mol}^{-1}$) < Cr ($\pm 10 \text{ kcal mol}^{-1}$).

3.3.2. Single Reference Systems. The density functionals considered in this study are all based on generalized KS theory⁷⁰ utilizing a single determinant description. The generalized KS DFT may fail for multireference molecular systems that contain degenerate or quasidegenerate orbitals/states. In a recent study,⁷¹ we investigated the multireference character of the ccCA-TM/11all set using several diagnostics including C_0^2 (the weight of leading configuration in a complete active space self-consistent field wave function), T_1 (the Frobenius norm of the coupled cluster t_1 amplitudes),^{72,73} D_1 (the matrix 2-norm of the coupled cluster t_1 amplitudes),^{74–76} spin contamination, and %TAE (percent total atomization energy).^{77,78} Using the criteria $T_1 < 0.05$, $D_1 < 0.15$, and %TAE < 10, as suggested in our earlier study,⁷¹ and $C_0^2 > 0.90$ (when the calculations are possible), 91 molecules (SR-91, see the list

in Supporting Information) are identified as single reference systems where the nondynamical correlation is not significant (Figure 3).

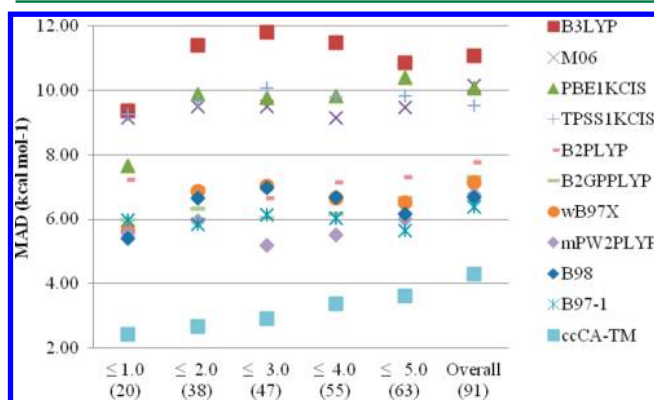


Figure 3. The DFT and ccCA-TM MADs (kcal mol^{-1}) for 91 single reference 3d transition-metal-containing molecules where nondynamical correlation is not significant.

The MADs of the 10 functionals decrease for the SR-91 subset, as compared to the MADs obtained for the overall ccCA-TM/11 set (Table 3). The magnitude of the improvement in the MADs varies for each functional. The MAD of ω B97X gives the largest decrease of $3.3 \text{ kcal mol}^{-1}$. The smallest decrease in MAD is found for TPSS1KCIS, only $0.3 \text{ kcal mol}^{-1}$. With the SR-91 set, as opposed to the ccCA-TM/11 set, the relative accuracy of the different suites of functionals can be further elucidated. As can be seen from Figure 3, B3LYP gives the largest overall MAD of $11.0 \text{ kcal mol}^{-1}$, followed by the three hybrid-meta-GGA functionals (M06: $10.1 \text{ kcal mol}^{-1}$; PBE1KCIS: $10.1 \text{ kcal mol}^{-1}$; TPSS1KCIS: $9.5 \text{ kcal mol}^{-1}$). The double hybrid functionals and the B97 family result in the smallest MADs in the range of $6.4\text{--}7.8 \text{ kcal mol}^{-1}$. The accuracy of the double hybrid functionals is in the decreasing order of mPW2-PLYP > B2GP-PLYP > B2-PLYP, and that of the three B97 functionals is B97-1 > B98 > ω B97X for the SR-91 set.

By applying more stringent diagnostic criteria, $T_1 < 0.05$, $D_1 < 0.10$, %TAE < 5, and $C_0^2 > 0.90$, a more refined set of 49 molecules (SR-49) than SR-91 is obtained to evaluate the performance of the functionals. We expected that possible multireference species, where severe nondynamical correlation may exist, are more effectively excluded from this SR-49 set as compared to SR-91. However, the diversity of SR-49 is also compromised due to the substantial decrease in the number of molecules, e.g., the pruned single reference set consists mainly of metal halides and no metal oxides. The MADs of most density functionals for the SR-49 set are further reduced as

Table 3. Mean Absolute Deviations (MAD; kcal mol^{−1}) of ΔH_f° 's Relative to Experimental Data for 3d Transition Metal Subcategories

# of molecules	SR ^a		MR ^b	coordination complexes	closed shell		open shell (multiplicity)				size (# of atoms)				ccCA-TM/11
							2	3	≥4	all	2	3	4	>5	
	91	49	25	25	67	64 ^c	33	26	67	126	75	36	18	66	193
B3LYP	11.1	8.5	11.2	30.6	22.4	19.7	6.1	8.1	9.1	8.1	6.4	7.7	10.5	23.9	13.1
B97-1	6.4	5.9	7.9	8.0	10.5	8.4	4.3	5.6	6.1	5.5	5.4	4.3	8.3	10.8	7.2
B97-1-DK ^d	7.1	7.2	7.9	7.3	9.1	7.7	4.8	6.3	6.5	6.0	5.6	4.6	8.5	10.0	7.1
ω B97X	7.1	5.1	12.4	17.5	16.2	12.8	6.7	8.0	7.4	7.4	8.0	6.6	7.8	15.8	10.4
B98	6.7	5.7	9.3	17.0	15.1	12.3	4.2	5.3	6.5	5.6	5.6	5.1	8.5	15.0	8.9
M06	10.1	8.9	10.8	11.6	16.1	13.5	6.9	9.4	8.7	8.4	7.3	9.2	15.6	15.4	11.0
PBE1KCIS	10.1	10.1	10.7	17.4	16.8	14.0	5.4	9.5	9.3	8.3	7.6	8.0	11.5	17.1	11.3
TPSS1KCIS	9.5	7.7	9.1	13.1	11.9	10.3	6.3	8.5	10.0	8.7	8.0	8.3	10.9	12.5	9.8
B2-PLYP ^e	7.8	5.7	10.9	15.6	15.6	12.2	6.7	10.2	7.5	7.8	6.2	8.8	8.3	14.7	9.6
B2GP-PLYP ^e	7.3	5.5	15.0	11.9	12.9	9.4	8.3	12.4	9.1	9.5	8.3	9.4	8.4	12.1	9.7
mPW2-PLYP ^e	6.8	5.0	9.3	8.2	9.4	7.0	6.3	7.1	7.9	7.3	5.6	7.2	7.0	9.8	7.3

^aSingle reference molecular systems where nondynamical correlation is not significant. ^bMolecular systems with strong multireference character except ScB₂, TiB, and VC. ^c⁷¹Cr₂, V₄O₁₀, and Cr₃O₉ are excluded. ^dThe second order Douglas–Kroll–Hess Hamiltonian was considered for the scalar relativistic effects. The cc-pVQZ-DK basis set was employed for the single point energies using the B97-1/cc-pVQZ geometries. ^eB3LYP/cc-pVQZ geometries and frequencies are used. Cr₂ is excluded.

compared to those for the SR-91 set. The MADs of double hybrid functionals are in the range of 5.0–5.7 kcal mol^{−1}, about 2.0 kcal mol^{−1} less than those for the SR-91 set. The MADs of B97-1, ω B97X, and B98 are 5.9, 5.1, and 5.7 kcal mol^{−1}, which are lower than those for the SR-91 set by 0.5, 2.0, and 1.0 kcal mol^{−1}, respectively. However, the PBE1KCIS MAD for the SR-49 set remains the same as that for the SR-91 set. The relative order of accuracy for the 10 functionals changes slightly from SR-91 to SR-49. Specifically, the B3LYP MAD (8.5 kcal mol^{−1}) is lower than that of hybrid-meta functionals M06 (8.9 kcal mol^{−1}) and PBE1KCIS (10.1 kcal mol^{−1}) for the SR-49 set. While the exact reasons for the large MADs of M06 and PBE1KCIS are not clear, the prediction of TM energetic properties by these two functionals should be treated with caution.

3.3.3. Multireference Subset.⁷⁹ A multireference (MR) subset was formulated to include 25 species where multireference character may be significant based on the diagnostics criteria $T_1 > 0.05$, $D_1 > 0.15$, and % TAE > 10 suggested in our earlier study.⁷¹ Metal dimers were not considered in this subset due to known difficulties in predicting properties of metal dimers by density functionals.^{14,80} The MADs of single hybrid density functionals for the MR set were compared to the respective MADs for the overall set (Table 3), and the changes in MAD were between −1.9 kcal mol^{−1} by B3LYP and +2.0 kcal mol^{−1} by ω B97X. However, the MADs of all density functionals decrease from the MR subset to the SR-49 subset, suggesting that a correlation may exist between the performance of density functionals and the significance of MR character. In contrast to the negative MSDs for SR-91 and SR-49 (Table S2 in Supporting Information), the MR subset is predicted with positive MSDs by all density functionals considered here except PBE1KCIS and TPSS1KCIS, which contain essentially no empirical parameter. The deficiency in recovering the substantial amount of nondynamical correlation in the MR set may result in the underestimation of binding energies by the density functionals with empirical parameters. Such errors cannot be compensated by introducing second

order perturbation theory based on generalized Kohn–Sham orbitals.

The MADs of B2-PLYP, mPW2-PLYP, and B2GP-PLYP for the MR subset are higher than the overall MADs by 1.3, 2.0, and 5.3 kcal mol^{−1}, respectively, and the differences are more pronounced when the comparisons are made between MR and SR subsets. The double hybrid functionals include both HF exchange and MP2-type correlation energy, which are sensitive to multireference character. B2GP-PLYP contains the largest relative amounts of MP2-type correlation energy (36%) and HF exchange (65%), and thus its performance deteriorates the fastest among the double hybrid functionals.

3.3.4. Coordination Complexes. There are 25 complexes such as Sc(C₅H₅)₃, Mn(CO)₅Cl, and Fe(CO)₄H₂ with coordinated bonds or organic ligands from the ccCA-TM/11 set. The determination of ΔH_f° 's for these types of complexes is important for the mechanistic elucidation of organic and bio-organic reactions where the metal complexes serve as model catalysts or reactants. B97-1 and mPW2-PLYP obtain the lowest MADs of 8.0 and 8.2 kcal mol^{−1}, respectively, while all other functionals yield MADs greater than 10 kcal mol^{−1} for the metal complex subset (Table 3), and B3LYP gives the largest MAD of 30.6 kcal mol^{−1}. In contrast to the similar MADs obtained by the three B97 functionals for the SR-91 and SR-49 sets, the MADs of B98 (17.0 kcal mol^{−1}) and ω B97X (17.5 kcal mol^{−1}) are much greater than that of B97-1. The double hybrid B2GP-PLYP (11.9 kcal mol^{−1}) gives a lower MAD than its parent B2-PLYP by 3.7 kcal mol^{−1}.

3.3.5. Multiplicity. The performance of functionals was examined for closed shell species (multiplicity = 1) and species with unpaired electrons (multiplicity > 1). There are 67 closed shell molecules in the ccCA-TM/11 set. For these molecules, the performance of each functional is similar to what was observed for the coordination complexes. The two smallest MADs are 9.4 kcal mol^{−1} with mPW2-PLYP and 10.5 kcal mol^{−1} with B97-1 (Table 3). This closed shell set includes the clusters V₄O₁₀ and Cr₃O₉ and the metal dimer Cr₂, which have the largest deviations for many functionals. (Cr₂ was already excluded for double hybrid functionals but not for the hybrid

and hybrid-meta functionals.) By removing these three molecules, the MADs for each functional are reduced by 1.6–3.5 kcal mol⁻¹. The MADs for 126 open shell molecules are lower than those obtained for closed shell species. The B97-1 and B98 functionals have the two lowest MADs of 5.5 and 5.6 kcal mol⁻¹, respectively. Compared to B3LYP, the double hybrid B2-PLYP and B2GP-PLYP did not show any improvement in MAD, suggesting that for open shell 3d TM species, the more computationally costly double hybrid functionals may not perform better than the single hybrid counterparts. To further investigate the effects of the number of unpaired electrons on the performance of density functionals, the open shell molecules are also considered with respect to one (doublet), two (triplet), and three or more (quartet or higher multiplicity) unpaired electrons. The set of doublets has the smallest MAD for all functionals, as compared with the sets of singlets and triplets. When open shell molecules in this study are grouped into doublets, triplets, and quartets or higher, the MADs from experimental values increase with the number of unpaired electrons for the functionals B97-1, B98, B3LYP, TPSS1KCIS, and mPW2-PLYP.

3.3.6. Molecular Size. The effect of molecule size (the number of atoms in the species) on the performance of the DFT functionals has been investigated (Table 3). In general, the MADs of most functionals increase as the size of molecule increases. However, such trends are changed or reversed among the subsets of diatomics, triatomics, and tetratomics for the B97 and double hybrid functionals. B97-1 yields the smallest MADs of 5.4 and 4.3 kcal mol⁻¹ for diatomics and triatomics, respectively, while mPW2-PLYP provides the best MADs for tetratomics and molecules of larger size.

3.4. Scalar Relativistic Effects. All above comparisons were based on DFT calculations utilizing the nonrelativistic Hamiltonian where scalar relativistic effects were omitted. However, the scalar relativistic effects can be significant for the theoretical predictions of ΔH_f° 's for 3d TM-containing species. For example, the scalar relativistic corrections were found in the range of -3.0 to 6.4 kcal mol⁻¹ at the MP2/cc-pVTZ-DK level,⁴⁴ where the second order Douglas–Kroll–Hess (DKH) Hamiltonian^{81,82} was employed. To assess the scalar relativistic effects, single point energy calculations by B97-1 were performed by using the second order DKH Hamiltonian in combination with the recontracted cc-pVQZ-DK basis sets.⁶⁴ The B97-1 functional was chosen since it showed the best overall performance among the functionals considered in this study. To differentiate from our nonrelativistic calculations, the calculations with the DKH Hamiltonian are denoted as B97-1-DK. Overall, the B97-1-DK shows the same accuracy as B97-1 (Table 3). For the subsets as given in Table 3, the B97-1-DK MADs are greater than the B97-1 MADs except for coordination complexes, closed shell molecules, and molecules of >5 atoms. Particularly, the B97-1-DK significantly reduced the absolute deviations from experimental values for oxide clusters V₄O₁₀ and (CrO₃)₃ by 12.8 and 29.0 kcal mol⁻¹, respectively. However, for single reference subsets SR-91 and SR-49, the B97-1-DK MADs are 7.1 and 7.2 kcal mol⁻¹, greater than the B97-1 MADs of 6.4 and 5.9 kcal mol⁻¹, respectively. It is thus suggested to use the DKH Hamiltonian (or other similar scalar relativistic treatment) when there are multiple metal centers for B97-1. Further investigation is warranted to examine if the utilization of the DKH Hamiltonian is beneficial for other density functionals.

4. CONCLUSIONS

The performance of 13 density functionals (B3LYP, B97-1, B97-2, ω B97X, ω B97X-D, B98, M06, PBE1KCIS, TPSS1KCIS, B2-PLYP, mPW2-PLYP, and B2GP-PLYP) for calculating the enthalpies of formation has been evaluated for the ccCA-TM/11 set of 193 3d TM molecules and various subsets with different electronic features.

This study confirms that, in general, B3LYP/cc-pVTZ geometries and frequencies can be used in combination with more sophisticated density functionals and/or larger basis sets, without adversely affecting the accuracy, in order to reduce the computational cost associated with TM thermochemistry.

Overall, B97-1 and the double hybrid mPW2-PLYP perform the best among the 13 functionals investigated. The double-hybrid functional mPW2-PLYP results are in closer agreement with the experimental data with uncertainties up to 3.0 kcal mol⁻¹, as opposed to the subsets with larger experimental uncertainties and the overall set. Similar trends are observed for the other two double hybrid functionals, B2-PLYP and B2GP-PLYP.

While B97-1 is optimal for V, Cr, Mn, Fe, and Ni, competitive functionals for the rest of the first row transition metals are TPSS1KCIS for Sc and Zn, B98 for Ti, PBE1KCIS for Co, and ω B97X for Cu. Double hybrid functionals are competitive in accuracy for V, Cr, and Co, but their computational cost is unfavorable as compared to single hybrid functionals.

For the two single reference subsets, SR-91 and SR-49, which are free of molecules where there might be severe non-dynamical correlation, the performances of the three B97 functionals and the double hybrid functionals are similar and are significantly better than that of the hybrid-meta-GGA functionals and B3LYP.

The performance of the functionals considered in this study is better for open shell molecules than for closed shell molecules. B97-1 and B98 result in the lowest MADs for open shell molecules, while mPW2-PLYP performs the best for closed shell molecules. Smaller MADs are obtained for doublet species than those with higher multiplicities.

Generally, the MADs of the density functionals are larger for subsets of bigger molecules. The B97-1 and B98 functionals perform the best for diatomics and triatomics, while the mPW2-PLYP functional yields the lowest MAD for molecules of four atoms or more.

In summary, our investigation on the performance of representative density functionals demonstrates the promising utilization of B97-1 and mPW2-PLYP for quantitative and reliable predictions of TM thermochemistry.

■ ASSOCIATED CONTENT

● Supporting Information

The atomic energies of transition metals by each density functional and basis set combination. The mean signed deviations of each density functional. The spin–orbit corrections (in kcal mol⁻¹) calculated by spin–orbit CI. Enthalpies of formation ($\Delta H_{f,298K}^\circ$) determined using the density functionals considered in this study for the ccCA-TM-11 set of 193 species or the truncated set of 180 species. The molecules of the SR-91, SR-49, and MR subsets. The listing of 25 coordination complexes. The molecular geometries optimized by B3LYP/cc-pVTZ for the ccCA-TM/11 set of 193

3d transition-metal-containing species. This material is available free of charge via the Internet at <http://pubs.acs.org>.

AUTHOR INFORMATION

Corresponding Author

*E-mail: akwilson@unt.edu.

Notes

The authors declare no competing financial interest.

ACKNOWLEDGMENTS

The authors gratefully acknowledge support from the National Science Foundation (Grant No. CHE-0809762). Local computer resources were, in part, provided via NSF (CHE-0741936) and by Academic Computing Services at the University of North Texas on the UNT Research Cluster. Grateful acknowledgements also go to the United States Department of Energy for support of the Center for Advanced Scientific Computing and Modeling (CASCaM).

REFERENCES

- (1) Cramer, C. J.; Truhlar, D. G. *Phys. Chem. Chem. Phys.* **2009**, *11*, 10757–10816.
- (2) Bühl, M.; Kabrede, H. J. *Chem. Theory Comput.* **2006**, *2*, 1282–1290.
- (3) Waller, M. P.; Braun, H.; Hojdis, N.; Bühl, M. J. *Chem. Theory Comput.* **2007**, *3*, 2234–2242.
- (4) Waller, M. P.; Bühl, M. J. *Comput. Chem.* **2007**, *28*, 1531–1537.
- (5) Bühl, M.; Reimann, C.; Pantazis, D. A.; Bredow, T.; Neese, F. J. *Chem. Theory Comput.* **2008**, *4*, 1449–1459.
- (6) Kulik, H. J.; Marzari, N. J. *Chem. Phys.* **2010**, *133*, 114103.
- (7) Jiménez-Hoyos, C. A.; Janesko, B. G.; Scuseria, G. E. *J. Phys. Chem. A* **2009**, *113*, 11742–11749.
- (8) Johnson, E. R.; Becke, A. D. *Can. J. Chem.* **2009**, *87*, 1369–1373.
- (9) Barden, C. J.; Rienstra-Kiracofe, J. C.; Schaefer, H. F., III. *J. Chem. Phys.* **2000**, *113*, 690–700.
- (10) Papas, B. N.; Schaefer, H. F., III. *J. Chem. Phys.* **2005**, *123*, 074321.
- (11) Jensen, K. P.; Roos, B. O.; Ryde, U. J. *Chem. Phys.* **2007**, *126*, 014103.
- (12) Uzunova, E. L. *J. Phys. Chem. A* **2011**, *115*, 1320–1330.
- (13) Gutsev, G. L.; Andrews, L.; Bauschlicher, C. W., Jr. *Theor. Chem. Acc.* **2003**, *109*, 298–308.
- (14) Gutsev, G. L.; Mochena, M. D.; Jena, P.; Bauschlicher, C. W., Jr.; Partridge, H., III. *J. Chem. Phys.* **2004**, *121*, 6785–6797.
- (15) Yao, C.; Guan, W.; Song, P.; Su, Z. M.; Feng, J. D.; Yan, L. K.; Wu, Z. J. *Theor. Chem. Acc.* **2007**, *117*, 115–122.
- (16) Song, P.; Guan, W.; Yao, C.; Su, Z. M.; Wu, Z. J.; Feng, J. D.; Yan, L. K. *Theor. Chem. Acc.* **2007**, *117*, 407–415.
- (17) Cheng, L.; Wang, M. Y.; Wu, Z. J.; Su, Z. M. *J. Comput. Chem.* **2007**, *28*, 2190–2202.
- (18) Hyla-Kryspin, I.; Grimme, S. *Organometallics* **2004**, *23*, 5581–5592.
- (19) Quintal, M. M.; Karton, A.; Iron, M. A.; Boese, A. D.; Martin, J. M. L. *J. Phys. Chem. A* **2006**, *110*, 709–716.
- (20) Zhao, Y.; Truhlar, D. G. *J. Chem. Phys.* **2006**, *124*, 224105.
- (21) Zhao, Y.; Truhlar, D. G. *Acc. Chem. Res.* **2008**, *41*, 157–167.
- (22) Li, S.; Hennigan, J. M.; Dixon, D. A.; Peterson, K. A. *J. Phys. Chem. A* **2009**, *113*, 7861–7877.
- (23) Mayhall, N. J.; Raghavachari, K.; Redfern, P. C.; Curtiss, L. A. *J. Phys. Chem. A* **2009**, *113*, 5170–5175.
- (24) Rinaldo, D.; Tian, L.; Harvey, J. N.; Friesner, R. A. *J. Chem. Phys.* **2008**, *129*, 164108.
- (25) Schultz, N. E.; Zhao, Y.; Truhlar, D. G. *J. Phys. Chem. A* **2005**, *109*, 4388–4403.
- (26) Schultz, N. E.; Zhao, Y.; Truhlar, D. G. *J. Phys. Chem. A* **2005**, *109*, 11127–11143.
- (27) Furche, F.; Perdew, J. P. *J. Chem. Phys.* **2006**, *124*, 044103.
- (28) Goerigk, L.; Grimme, S. *J. Chem. Theory Comput.* **2011**, *7*, 291–309.
- (29) Cundari, T. R.; Leza, H. A. R.; Grimes, T.; Steyl, G.; Waters, A.; Wilson, A. K. *Chem. Phys. Lett.* **2005**, *401*, 58–61.
- (30) Xu, X.; Truhlar, D. G. *J. Chem. Theory Comput.* **2012**, *8*, 80–90.
- (31) Riley, K. E.; Merz, K. M. *J. Phys. Chem. A* **2007**, *111*, 6044–6053.
- (32) Yang, Y.; Weaver, M. N.; Merz, K. M., Jr. *J. Phys. Chem. A* **2009**, *113*, 9843–9851.
- (33) Tao, J.; Perdew, J. P.; Staroverov, V. N.; Scuseria, G. E. *Phys. Rev. Lett.* **2003**, *91*, 146401.
- (34) Toulouse, J.; Savin, A.; Adamo, C. *J. Chem. Phys.* **2002**, *117*, 10465–10473.
- (35) Jiang, W.; DeYonker, N. J.; Determan, J. J.; Wilson, A. K. *J. Phys. Chem. A* **2012**, *116*, 870–885.
- (36) Tekarli, S. M.; Drummond, M. L.; Williams, T. G.; Cundari, T. R.; Wilson, A. K. *J. Phys. Chem. A* **2009**, *113*, 8607–8614.
- (37) The experimental uncertainties of enthalpies of formation for transition-metal-containing molecules are relatively large. In our earlier study, the average experimental uncertainty for 17 transition-metal-containing molecules was about 3.0 kcal mol⁻¹. The transition metal accuracy was suggested as ± 3.0 kcal mol⁻¹. See ref 35 for more details.
- (38) Zhao, Y.; Truhlar, D. G. *Theor. Chem. Acc.* **2008**, *120*, 215–241.
- (39) Hamprecht, F. A.; Cohen, A. J.; Tozer, D. J.; Handy, N. C. *J. Chem. Phys.* **1998**, *109*, 6264–6271.
- (40) Curtiss, L. A.; Raghavachari, K.; Redfern, P. C.; Pople, J. A. *J. Chem. Phys.* **1997**, *106*, 1063–1079.
- (41) Curtiss, L. A.; Redfern, P. C.; Raghavachari, K. *J. Chem. Phys.* **2005**, *123*, 124107.
- (42) DeYonker, N. J.; Grimes, T.; Yockel, S.; Dinescu, A.; Mintz, B.; Cundari, T. R.; Wilson, A. K. *J. Chem. Phys.* **2006**, *125*, 104111.
- (43) DeYonker, N. J.; Wilson, B. R.; Pierpont, A. W.; Cundari, T. R.; Wilson, A. K. *Mol. Phys.* **2009**, *107*, 1107–1121.
- (44) DeYonker, N. J.; Peterson, K. A.; Steyl, G.; Wilson, A. K.; Cundari, T. R. *J. Phys. Chem. A* **2007**, *111*, 11269–11277.
- (45) DeYonker, N. J.; Williams, T. G.; Imel, A. E.; Cundari, T. R.; Wilson, A. K. *J. Chem. Phys.* **2009**, *131*, 024106.
- (46) Kohn, W.; Becke, A. D.; Parr, R. G. *J. Phys. Chem.* **1996**, *100*, 12974–12980.
- (47) Stephens, P. J.; Devlin, F. J.; Chabalowski, C. F.; Frisch, M. J. *J. Phys. Chem.* **1994**, *98*, 11623–11627.
- (48) Becke, A. D. *J. Chem. Phys.* **1997**, *107*, 8554–8560.
- (49) Schmider, H. L.; Becke, A. D. *J. Chem. Phys.* **1998**, *108*, 9624–9631.
- (50) Wilson, P. J.; Bradley, T. J.; Tozer, D. J. *J. Chem. Phys.* **2001**, *115*, 9233–9242.
- (51) Chai, J.-D.; Head-Gordon, M. *J. Chem. Phys.* **2008**, *128*, 084106.
- (52) Chai, J.-D.; Head-Gordon, M. *Phys. Chem. Chem. Phys.* **2008**, *10*, 6615–6620.
- (53) Perdew, J. P.; Burke, K.; Ernzerhof, M. *Phys. Rev. Lett.* **1996**, *77*, 3865–3868.
- (54) Grimme, S. *J. Chem. Phys.* **2006**, *124*, 034108.
- (55) Schwabe, T.; Grimme, S. *Phys. Chem. Chem. Phys.* **2006**, *8*, 4398–4401.
- (56) Perdew, J. P.; Schmidt, K. *AIP Conf. Proc.* **2001**, *577*, 1–20.
- (57) Karton, A.; Tarnopolsky, A.; Lamere, J. F.; Schatz, G. C.; Martin, J. M. L. *J. Phys. Chem. A* **2008**, *112*, 12868–12886.
- (58) Görling, A.; Levy, M. *Phys. Rev. B* **1993**, *47*, 13105–13113.
- (59) Sharkas, K.; Toulouse, J.; Savin, A. *J. Chem. Phys.* **2011**, *134*, 064113.
- (60) Frisch, M. J.; Trucks, G. W.; Schlegel, H. B.; Scuseria, G. E.; Robb, M. A.; Cheeseman, J. R.; Scalmani, G.; Barone, V.; Mennucci, B.; Petersson, G. A.; Nakatsuji, H.; Caricato, M.; Li, X.; Hratchian, H. P.; Izmaylov, A. F.; Bloino, J.; Zheng, G.; Sonnenberg, J. L.; Hada, M.; Ehara, M.; Toyota, K.; Fukuda, R.; Hasegawa, J.; Ishida, M.; Nakajima, T.; Honda, Y.; Kitao, O.; Nakai, H.; Vreven, T.; Montgomery, J. A., Jr.; Peralta, J. E.; Ogliaro, F.; Bearpark, M.; Heyd, J. J.; Brothers, E.; Kudin, K. N.; Staroverov, V. N.; Kobayashi, R.; Normand, J.; Raghavachari, K.; Rendell, A.; Burant, J. C.; Iyengar, S. S.; Tomasi, J.; Cossi, M.; Rega,

N.; Millam, J. M.; Klene, M.; Knox, J. E.; Cross, J. B.; Bakken, V.; Adamo, C.; Jaramillo, J.; Gomperts, R.; Stratmann, R. E.; Yazyev, O.; Austin, A. J.; Cammi, R.; Pomelli, C.; Ochterski, J. W.; Martin, R. L.; Morokuma, K.; Zakrzewski, V. G.; Voth, G. A.; Salvador, P.; Dannenberg, J. J.; Dapprich, S.; Daniels, A. D.; Farkas, Ö.; Foresman, J. B.; Ortiz, J. V.; Cioslowski, J.; Fox, D. J. *Gaussian 09*, Revision A.1; Gaussian, Inc.: Wallingford, CT, 2009.

(61) Dunning, T. H., Jr. *J. Chem. Phys.* **1989**, *90*, 1007–1023.

(62) Woon, D. E.; Dunning, J. T. H. *J. Chem. Phys.* **1993**, *98*, 1358–1371.

(63) Wilson, A. K.; Woon, D. E.; Peterson, K. A.; Dunning, J. T. H. *J. Chem. Phys.* **1999**, *110*, 7667–7676.

(64) Balabanov, N. B.; Peterson, K. A. *J. Chem. Phys.* **2005**, *123*, 064107.

(65) Laury, M. L.; Boesch, S. E.; Haken, I.; Sinha, P.; Wheeler, R. A.; Wilson, A. K. *J. Comput. Chem.* **2011**, *32*, 2339–2347.

(66) Ochterski, J. W. *Thermochemistry in Gaussian*. http://www.gaussian.com/g_whitepap/thermo.htm (accessed 06/27/2011).

(67) Johnson, E. R.; Dickson, R. M.; Becke, A. D. *J. Chem. Phys.* **2007**, *126*, 184104.

(68) Wang, N. X.; Wilson, A. K. *J. Chem. Phys.* **2004**, *121*, 7632–7646.

(69) Abrams, M. L.; Sherrill, C. D. *J. Chem. Phys.* **2004**, *121*, 9211–9219.

(70) Kohn, W.; Sham, L. J. *Phys. Rev.* **1965**, *140*, A1133–A1138.

(71) Jiang, W.; DeYonker, N. J.; Wilson, A. K. *J. Chem. Theory Comput.* **2012**, *8*, 460–468.

(72) Lee, T. J.; Taylor, P. R. *Int. J. Quant. Chem. Symp.* **1989**, *S23*, 199–207.

(73) Lee, T. J.; Rice, J. E.; Scuseria, G. E.; Schaefer, H. F. *Theor. Chim. Acta* **1989**, *75*, 81–98.

(74) Leininger, M. L.; Nielsen, I. M. B.; Crawford, T. D.; Janssen, C. L. *Chem. Phys. Lett.* **2000**, *328*, 431–436.

(75) Janssen, C. L.; Nielsen, I. M. B. *Chem. Phys. Lett.* **1998**, *290*, 423–430.

(76) Lee, T. J. *Chem. Phys. Lett.* **2003**, *372*, 362–367.

(77) Karton, A.; Rabinovich, E.; Martin, J. M. L.; Ruscic, B. *J. Chem. Phys.* **2006**, *125*, 144108.

(78) Karton, A.; Daon, S.; Martin, J. M. L. *Chem. Phys. Lett.* **2011**, *510*, 165–178.

(79) A reviewer has pointed out that it would be useful to construct a subset of 3d transition-metal-containing species with strong multi-reference character.

(80) Gutsev, G. L.; Bauschlicher, C. W. *J. Phys. Chem. A* **2003**, *107*, 4755–4767.

(81) Douglas, M.; Kroll, N. M. *Ann. Phys. (NY)* **1974**, *82*, 89–155.

(82) Hess, B. A. *Phys. Rev. A: Gen. Phys.* **1986**, *33*, 3742–3748.